Gabriel Rovina

March – July 2015

RESEARCH INTERNSHIP REPORT

Numerical simulations of the electrical activity of the left ventricle for the cardiac resynchronisation therapy

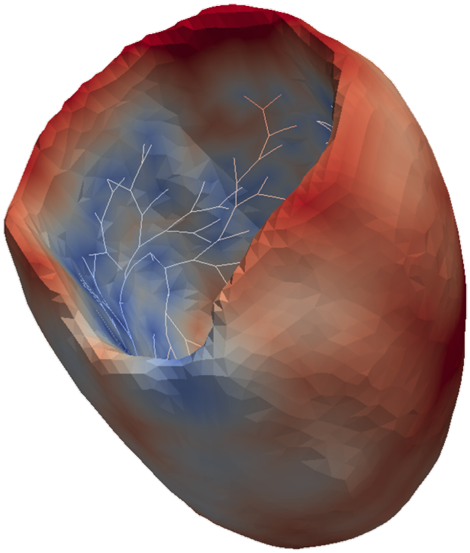

Supervision: Christian Vergara
Luca Formaggia

Laboratory for Modelling and Scientific Computing
Department of Mathematics
Politecnico di Milano, Italy

Contents

Cover image: simulation of a healthy activation (same as in Figure 12).

1 Introduction

Cardiac Resynchronisation Therapy (CRT) is a treatment applied under some specific clinical pictures involving malfunctioning of the heart's conduction system. Nowadays, a series of criteria established by the New York Heart Association determine when CRT should be applied and when should it not.

For cases responding to the therapy, patient's quality of life may be valuably improved, increasing his or her tolerance to exercises and reducing the number of hospitalisations and mortality. However, the rate of non-responders lies near one-third [Romero et al., 2010; Yu et al., 2005], representing the investment of a great amount of resources for no significant benefits in return.

In the light of this problematic but promising scenario, a better understanding of these pathological behaviours and of how CRT interferes in the heart's electrical activation is strongly desirable. This study's main goal is to work on this field of research, contributing to the future establishment of effective guidelines for CRT.

This work *stands on the shoulders of* [Palamara, 2014] and [Savaré, 2014]. In addition, it wouldn't be possible without the inestimable cooperation of the Division of Cardiology from the Santa Maria del Carmine hospital – Rovereto, Italy. Following the new CRT techniques adopted in Rovereto, a kick off for incorporating EnSite NavX data into the current models was given.

In what concerns the contributions to previous studies, this work comprehends the optimisation and revision of the main simulation codes, development of new features, as well as the implementation of new scripts such as the one for applying the image inpainting functions and the reconstruction of a real ventricle from MRI data.

2 Background

This section is dedicated to providing the reader with some general information on the cardiac electrical functioning and some of the most common diseases related to the conduction system.

2.1 Heart's electrical activity

The healthy cardiac stimulation consists of three major phases: the generation of an electrical signal, its distribution and its effect upon the muscular fibres.

All the components of this system play precise roles and are thus very specialised. Also for this reason, a reliable computational model of the heart must take into account a series of different components.

The signal responsible for the whole activation starts off at the **sinoatrial node**, heart's natural pacemaker. This specialised group of cells, located on the wall of the right atrium, is capable of depolarising itself spontaneously and in a synchronous way.

Depolarisation wave reaches the atria, first muscular set to be stimulated, and the **atrioventricular node** (see Figure 1). This second node is responsible for delaying the electrical signal before it gets to the ventricles, giving time for the atria to contract, properly filling the ventricular cavities.

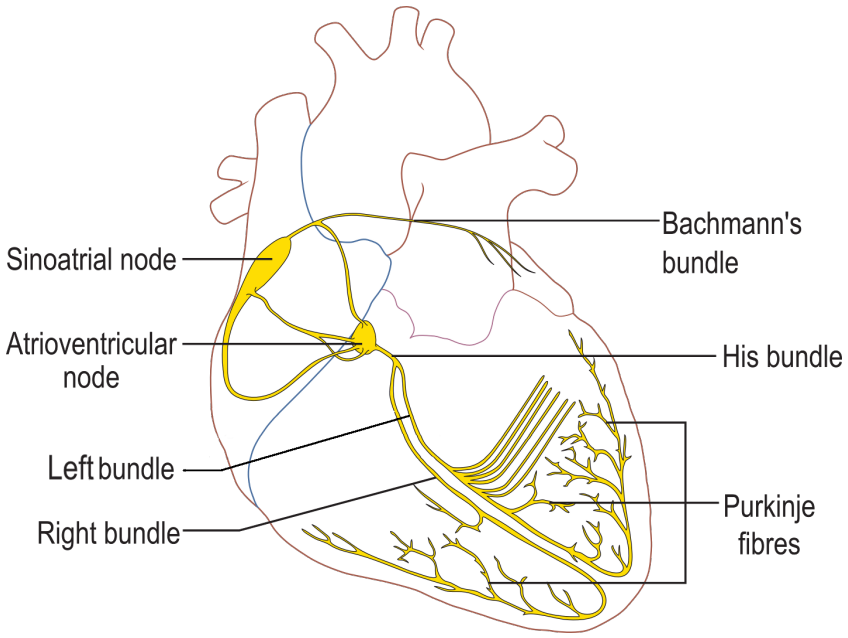

Figure 1: Heart's conduction system

The signal then follows its path via the **His bundle** and is derived into the **left and right bundles**. These fibres extend themselves toward the *a*pex[1] of the ventricles, neighbouring the

[1] the tip of the heart (*i.e.* its most inferior part)

*s*eptum[2], and gradually branch to become a complex fibrous network firstly described by J. E. Purkynje in 1839.

The Purkynje network, as it is known, spreads along the internal wall of the ventricles – more precisely, the subendocardial layer. The fibres are responsible for quickly distributing the electrical stimulus along the ventricular musculature, yielding synchronism and thus efficiency to the contraction. In order to transfer the electrical stimulus from the conduction system to the muscle, the signal traverses specialised neuromuscular junctions, called the Purkinje-Muscle Junctions (PMJ).

In a healthy scenario, the signal comes from the network and traverses the PMJ to arrive to the muscle; this is called the **orthodromic propagation**. When passing through the PMJ, orthodromic propagation delays the signal of about 5 ms.

However, if external sources are present, such as a pacemaker or a differentiated part of the muscular tissue, the signal may come from the muscle to the network, flowing in the reverse direction; this is called the **antidromic propagation**. The delay added to the wave front is lower in this case: its value is about 3 ms.

Either in one sense or another, the electrical signal may be spread throughout the ventricle and activates the cardiac tissue, inducing the contraction. After depolarisation and contraction, the muscular tissues slowly regain their quiescent electrical potential and become able to receive another stimulus. The complete cardiac activation takes about 0.6 seconds [Netter and Yonkman, 1981].

2.2 Diseases related to the conduction system

When a part of the conduction system is compromised, the whole propagation in the heart may be altered. For many cases, it may induce ventricular dyssynchrony.

Indeed, the left ventricle is the main actor of the cardiac pumping, and therefore amidst the most important parts regarding the necessity of clinical intervention. Also for CRT that will be the case.

Considering the precise way in which the stimulus is distributed along the heart, deviations from its natural functioning may be synonyms of *atrio-*, *inter-* or *intra-* **ventricular desynchronies** – respectively between atrium and ventricle; left and right ventricles and within a single ventricle.

As a consequence, the irregular contraction can lead to efficiency loss, low resistance to exercises and a series of risks to the patient.

2.2.1 Bundle branch block

Under some conditions such as arteriosclerosis[3], infarction[4] and ventricle overcharging, the bundles deriving from the His one may be injured [Netter and Yonkman, 1981], affecting the propagation of stimuli. This clinical picture is known as a bundle branch block and strongly alters the depolarisation chain. It is one of the main causes of ventricular dyssynchrony.

[2] dividing wall between right and left chambers
[3] thickening and hardening of arterial walls
[4] tissue death caused by obstruction of blood supply

In this case, the signal – normally reaching the muscle through the Purkinje network – may come from alternative paths or not come at all, depending on the position and on the extension of the damaged region.

Commonly, the signal is still able to propagate through the unblocked bundle, reach the respective bundle's ventricle and be tardively transferred to the other ventricle via muscular means. Evidently, the transport velocity in the muscular cells is slower than in the specialised conduction system, the ratio between the two being about 5 to 10 times [Kerckhoffs et al., 2003].

This study is mainly interested in the cases of Left Bundle Branch Block (LBBB), in which the left ventricle is the most affected one.

2.2.2 Wolff-Parkinson-White syndrome

Inversely to the case of blocked conduction paths, irregularities in the heart beat may be caused by the presence of additional ways of propagation.

Normally connecting the left atrium to the left ventricle, an extra bundle called *bundle of Kent* may transport the signal to the left ventricle prematurely, inducing premature excitation.

As a consequence, intraventricular dyssynchrony may take place and, in accentuated cases, the syndrome may also be related to ventricular fibrillation[5] and can even lead to sudden death.

2.3 The cardiac resynchronisation therapy

Among the treatments for ventricular dyssynchrony, the implantation of an appropriate pacemaker is one of the most efficient. The CRT consists of the artificial stimulation of the heart by means of two or more leads positioned in the right ventricle (on the endocardium) and on the left one (in the coronary veins) and alternatively a third one, in the right atrium. The three of them can be seen in Figure 2.

In addition to resynchronising electrical activation, a variation of the CRT devices called CRT-D also incorporates a defibrillator artefact. This series of pacemakers are able to recognise a cardiac fibrillation and apply an electrical charge in order to revert it. This is the particular case in Figure 2b, in which the right atrial lead is thicker due to the presence of the defibrillator.

The standard clinical criteria for implementing a device as such follow nowadays the orientations from the New York Heart Association: left ventricular end-diastolic diameter greater than 55 mm, ejection fraction (also in the left-ventricle) lower than 35 % and prolonged QRS complex[6] interval on electrocardiogram (> 120 ms) Tobon-Gomez et al. [2013].

Be that as it may, clear guidelines for CRT implantation are not yet well established [Reumann et al., 2007] and precise patient selection also remains a challenging issue [Tobon-Gomez et al., 2013], as denounces the accentuated ratio of patients that do not present benefits from the treatment (*i.e.*, the non-responders).

[5] uncoordinated contraction; quivering

[6] Set of waves in the electrocardiogram corresponding to the depolarisation of the left ventricle

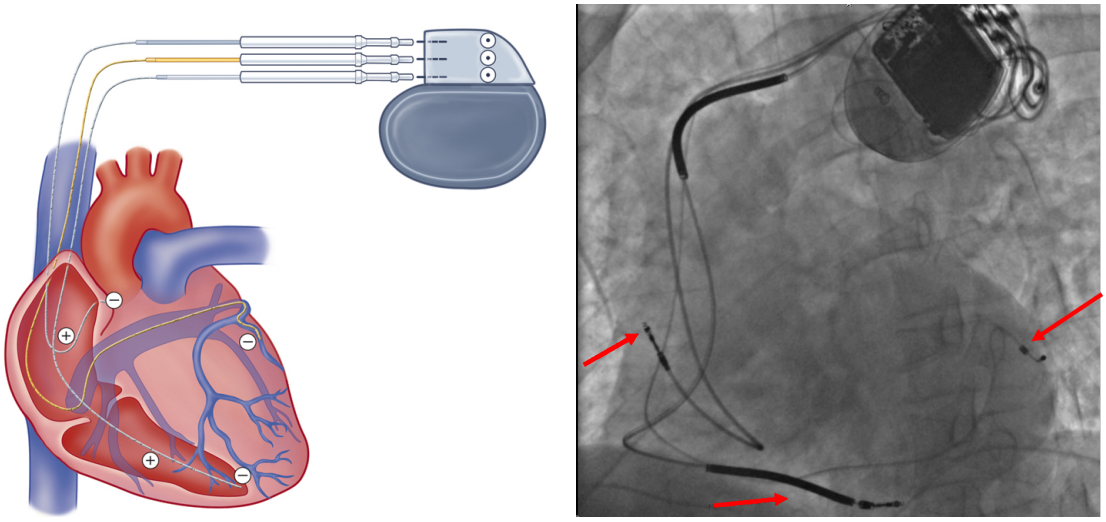

(a) (b)

Figure 2: Pacemaker leads in CRT-D
From left to right: right atrial, right ventricle and left ventricle leads.
Illustration (a) taken from http://www.clevelandclinicmeded.com

2.3.1 Positioning and timing

One of the most problematic tasks in CRT is defining the most adequate position for the leads, along with setting up the time gap between them. Thanks to the collaboration of the Division of Cardiology from the Santa Maria del Carmine hospital (Rovereto, Italy), a CRT implantation could be attended. Not only it was an opportunity to understand how the intervention is performed, but also to identify what are the practical needs from clinicians' perspective.

The right ventricle catheter is normally placed in the apical part of that chamber [Blanc et al., 1997; Butter et al., 2000]. According to the clinicians in Rovereto, criteria for positioning the left-ventricle lead depends on the case, for the geometry of the coronary veins and the activation pattern may change considerably from one patient to another.

In the Santa Maria del Carmine hospital, clinicians were assisted by the EnSite NavX system (St. Jude Medical Inc., Minnetonka, MN, USA). It consists of a mapping platform able to generate live images of the geometry and electrical data, permitting them to find the eligible veins for the pacing site and to visualise the order in which regions are activated.

In general, the optimal positioning is determined from a trade-off between the eligibility of the vein – calibre, geometry, accessibility – and lateness of the activation in the region. An ideal place would be a lately activated and easily accessible one. According to the clinicians, if a such a site or similar position are not available, the CRT may be abandoned.

A second step, when pacing sites are available, consists of adjusting the leads timings. Best configurations are chosen aiming a narrower QRS complex in the patient's electrocardiogram.

In this context, the motivations of this work lie on trying to contribute to the development of CRT by providing a better understanding of the cardiac electrical behaviour. For this purpose, simulations of the activation patterns of the left ventricle for different scenarios are carried.

3 Modelling

3.1 Geometry

3.1.1 Myocardium

It is medical routine to acquire radiological images when implanting a CRT device is being considered. Imagery can provide clinicians with more information on the patient's cardiac functioning – such as the ejection fraction – and an overview of the region where the intervention may take place.

In this study, clinical images were treated and a complete three-dimensional reconstruction of the left ventricle was performed. The process of carving the desired geometry out of this data is called image segmentation.

Metal artefact reduction In the case of a patient with a pacemaker of other implanted artefacts, captured images present alterations due to the presence of metallic components. Before performing segmentation, images should be treated in order to reduce the perturbations introduced by these artefacts. To perform this task in this study, we developed a new MATLAB routine, able to read image data exported from radiology and treat them. It uses the linear inpainting function implementation from [Faggiano et al., 2014]. Figure 3 compares a sample before and after inpainting.

Segmentation The segmentation procedure comprehends several steps and, although some automatised techniques can be of great use, they are far from providing more than an initial help for the majority of the cases. ITK-SNAP [Yushkevich et al., 2006] was the software used in this research for image segmentation. Different segmented elements where then composed and treated with Blender [Blender Online Community, 2015].

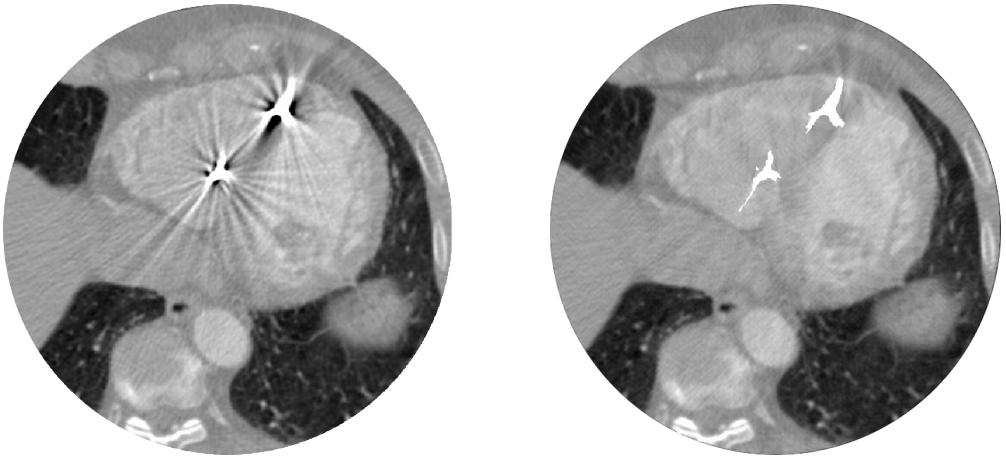

(a) Original (b) Inpainted

Figure 3: Metal artefact reduction by linear inpainting

Region competition In ITK-SNAP, the first step consists of a semi-automatised technique called *Region competition*. One starts by specifying threshold values for the pixels defining the area one is interested in. This is followed by a "bubble expansion" process, in which spheres are placed inside the region and expand respecting the borders of the thresholded image, as well as a smoothing factor (see Figures 4a – 4c). As image 4 shows, starting from the manually positioned bubbles, the algorithm expands their domain based on image contrast (region competition) and smoothing criteria. It works relatively well, but can "leek" to other regions if ever contrast or image quality are not sufficiently clear. In the case presented above, segmentation finished by expanding to a part outside of the ventricle itself (in Figure 4c, on the right side). This anomaly – as well as other small holes and contour issues – was corrected manually, as one can observe in Figure 4d.

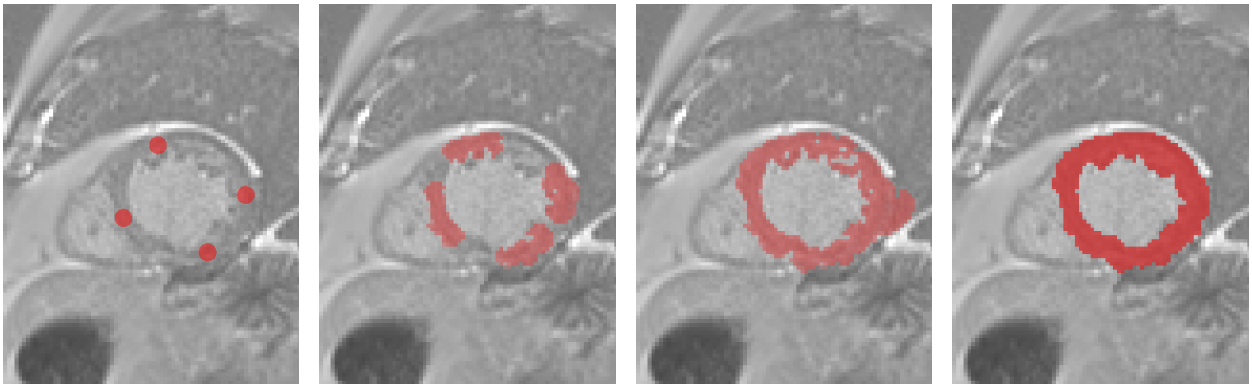

(a) Initial (b) Expansion (c) Final (d) Manual

Figure 4: Region competition technique in ITK-SNAP

Manual segmentation Region competition is useful for an initial, coarser approximation of the aimed region. However, as in most cases images are not sufficiently clear to permit a completely automatised segmentation, manual work is often required in order to obtain an appreciable result. These adjustments consist of manually specifying ("painting") the region of interest on the original clinical images, slice by slice. This process is able to generate good results, but can be considerably time-consuming depending on the number of image slices (the number can vary from a dozen slices to few hundred). An example of manual adjustments is given in Figure 4d, corrected manually from Figure 4c.

Smoothing Once the region is segmented, a smoothing step is necessary in order to reduce small-scale perturbations and noise. This process can be performed in ITK-SNAP before exporting the mesh. Nevertheless, some extra, fine adjustments where executed in Blender. However, smoothing steps must not be undertaken exaggeratedly, for one risks sweeping important geometrical information in the process and thus losing reliability to original data. After some parameter tuning such as the number of iterations and the relaxation factors, the results obtained are presented in Figure 5. We could then reload the smoothed geometry superposed

to original image data in order to confirm the model was still an accurate representation of the left ventricle.

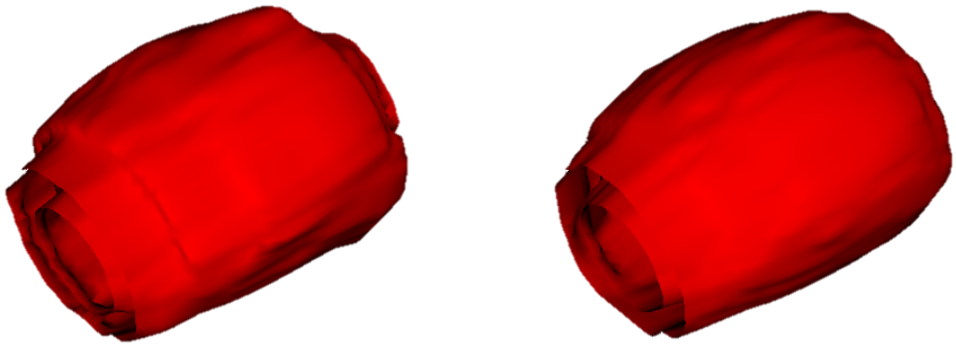

(a) Original (b) Smoothed

Figure 5: Mesh smoothing
The image above shows the results of the smoothing process applied to the first of two segmented parts.

Final geometry For the specific case studied in this work, no sequence of images in the magnetic resonance data contained the whole left ventricle. Therefore, it was necessary to perform two different, complementary segmentations and then merge them in a second step through a laborious handwork in Blender.

Once the geometry was reconstructed, its tetrahedral mesh was generated following constraints on the volume and degeneration of the elements. The final, merged geometry and its mesh are shown in Figure 6.

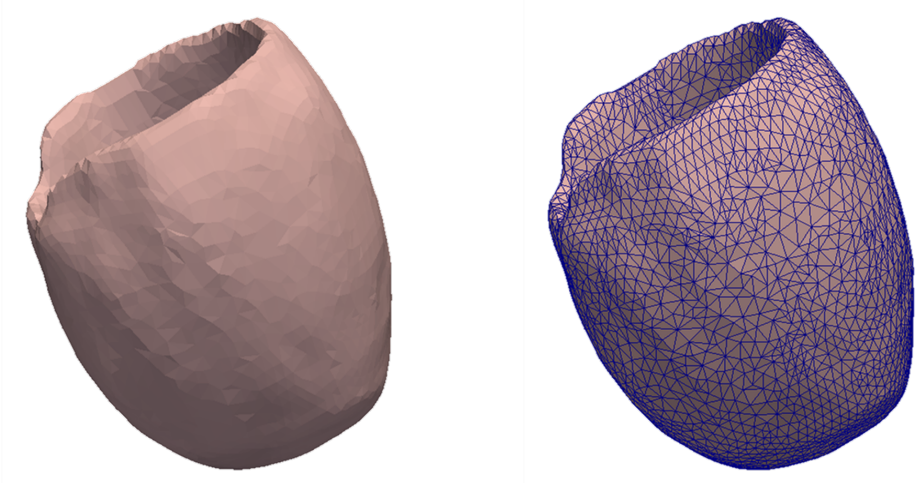

(a) (b)

Figure 6: Final segmented left ventricle
The mesh has approximately 84000 cells and 15000 points

3.1.2 Purkinje network

Conversely to the myocardium, the Purkinje network is not visible with regular imagery techniques. For this reason, the fibre distribution is generated from a randomised algorithm following a fractal bifurcation rule [Ijiri et al., 2008]. Parameters are defined statistically, following biological data and background research.

The Purkinje network extends itself along the major part of the endocardium, but few or no ramifications are present near the bundle branches (Figure 1). In order to take into account this physiological aspect, the septum region must defined during the generation of the network. Other parameters include the locations of the His and left bundles, as well as some of their main bifurcations.

In addition, a plan defining dividing the main body of the ventricle from its base is defined. On the upper, basal region, no ramifications are present. Finally, the number of bifurcation layers and other dimensioning inputs are set and the network is generated. The result is shown in Figure 7.

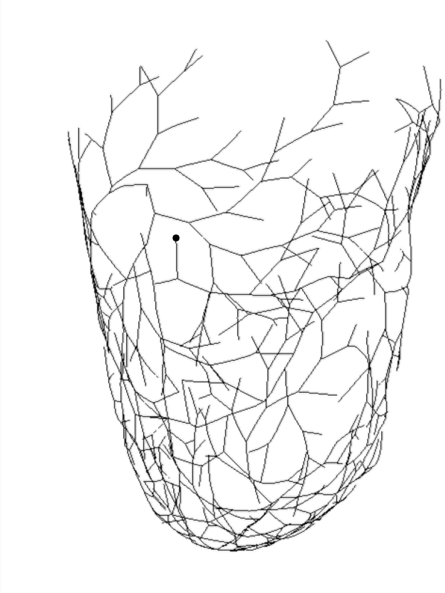

Figure 7: Generated Purkinje network

Here, a bullet dot was added to represent the network starting point for the case of a healthy propagation, *i.e.*, the point on the endocardium fibres closest to the atrioventricular node.

The works from [Palamara et al., 2014] and [Vergara et al., 2014] offer a method for calculating a patient-specific network from the statistically generated one. In other words, they propose a method for adapting the generated network's PMJ positions in order to make it provide an electrical activation result as close as possible to the collected electrical activation data on the endocardium.

Unfortunately, the adaptation of a tentative network to patient-specific one is entirely dependent of electrical activation data from the left ventricle endocardium. This sort of acquisition is only performed in cases of strong need, given that it implies accessing the high pressure routes

and the left ventricle itself.

3.1.3 EnSite NavX

In what concerns the EnSite Navx system, a MATLAB script was written in order to reconstruct the coronary geometry from the exported files provided by the Division of Cardiology from the Santa Maria del Carmine hospital. The routine reads geometrical data and generates a three dimensional mesh of the visited areas: normally the coronary sinus, the right atrium and ventricle and some of the neighbouring veins.

The result produced by the code for the studied case is shown in Figure 8

Figure 8: Coronary geometry reconstructed from EnSite NavX data
Clinicians mapped the main coronary veins and also the right atrium and ventricle.

3.2 Modelling the electrical propagation

Once the geometry is defined, a model for the electrical propagation must be established. It must not only be able to represent conduction in both the Purkinje fibres and the myocardium, but also account for the coupling between these two domains.

For the scope of this work, a reasonable approach seemed to be modelling the propagation in the network and in the ventricle as Eikonal problems, respectively in one and three dimensions. The coupling issue will be discussed in the sequence.

Other models are present in the literature, such as the physiological and phenomenological ones, based on the estimation of ionic levels and exchanges through cellular walls. However, they can be extremely time-consuming in both execution and implementation.

Although the Eikonal one may be limited to describing the macroscopic behaviour – not accounting for detailed cellular dynamics –, it does offer good performance and reliable solutions

in what concerns the activation times (*i.e.*, the time when the wave front arrives at that point), therefore meeting the needs of this work.

3.2.1 Eikonal equation

Taking into consideration that the propagation in the studied tissues is mainly advective [Palamara, 2014], one may want to start from the non-diffusive Eikonal equation for a domain $\Omega \subset \mathbb{R}^n$ – in our case, Ω can be the myocardium or the network. It reads as follows:

$$C\sqrt{\nabla u\, D\, \nabla u^t} = 1 \qquad \text{in } \Omega, \tag{1}$$

where u is the unknown activation time in Ω; C is a conductivity (possibly space-dependent) parameter and D is a rotation matrix that accounts for the direction of fibres (*i.e.*: anisotropy).

An interpretation of Equation 1 is that the modulus of the propagation velocity in a point x of Ω is given by $1/C$. Hence, higher values of C would correspond to injured regions and infarction scars, while smaller ones would represent healthy regions and specialised fibres.

This model is applied to both the network and the myocardium. However, for the unidimensional case of the Purkinje network, Equation 1 simplifies to:

$$C\left|\frac{du}{ds}\right| = 1 \qquad \text{in } \Omega, \tag{2}$$

for s being the coordinates along the network.

For each problem (in the network and in the myocardium), the model is completed by the insertion of appropriate boundary conditions in the following explicit form:

$$u = u_o \qquad \text{in } \Gamma, \tag{3}$$

for Γ being the set of points where the solution is known.

3.2.2 Numerical solution of the Eikonal problem

The algorithms used for solving the Eikonal equation are those called the Fast Marching Methods (FMM), originally from [Sethian, 1999].

The principle behind these methods is the observation that, for the propagation of a signal in time, higher values can not influence lower ones (the past). Therefore, one can always be sure of the minimum values and solution can be propagated from a set of known points by hopping through neighbouring minima.

Taking this into consideration, [Sethian, 1999] proposes the definition of three sets: the **accepted**, the **trial** and the **far** points. The former consisting of the points where solution have been determined (initially coinciding with the starting points, Γ); the trial being the points neighbouring the accepted ones; and the latter being consisted of the remaining points.

Taking the isotropic case as an example, the algorithm starts by setting the known points (boundary conditions) as the accepted and the trail ones.

The trial point with the minimum value is then selected and moved to accepted. Its trial and far neighbours are updated by adding a time value equivalent to the distance between the

points divided by the velocity of propagation in that region. Therefore, being Y the point neighbouring an accepted one and keeping in mind Equation , the computation for updating the solution in Y writes:

$$u_Y = \min(u_Y, u_X + C\ ||X - Y||_2)\,, \tag{4}$$

This means that the solution in Y only changes in the case that X lower value to offer. Once the solution is initialized following Equation 4 in a point that belonged to the far domain, this point is moved to the trial set.

Once all trial and far neighbours are updated (and have become all trial), the process is repeated for the next minimum value of a trial point. As a consequence, the neighbouring border marches outwards until the moment when there are no trial points left. Figure 9 illustrates a moment in propagation.

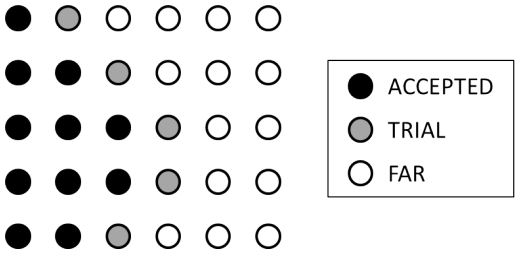

Figure 9: Propagation with the FMM

From these definitions, a pseudo-code for the FMM is written in Algorithm 1.

This algorithm is applied to solve the Eikonal problem in both of the domains. However, for the particular case of anisotropic propagation, in which the gradient does not necessarily coincide with characteristic directions, some recursive corrections are introduced in order to provide a precise solution, following the description that can be found in [Konukoglu et al., 2007]. This extra step consists of re-updating the solution for *all* the neighbours of a newly-accepted point, including those already marked as accepted.

3.2.3 Coupling between domains

Once the numerical solution to the Eikonal equation is described, the main matter becomes the coupling between the solutions in the two domains: how activation in the network affects the solution on the myocardium and vice-versa. The proposed algorithm [Palamara et al., 2014; Vergara et al., 2014] for solving the coupled problem relies on the following hypothesis.

Hypothesis No "second degree" antidromic activation takes place. By second degree antidromic activation, one should understand the case in which a signal coming from the myocardium, entering the network via antidromic propagation, then coming back to the myocardium and finally re-entering the network. Indeed, as the propagation within the network is 5 to 10 times faster than myocardial muscular tissue [Kerckhoffs et al., 2003] and there is a delay of some milliseconds added in each passage through a PMJ, it becomes very improbable

Algorithm 1 Fast marching method

```
ACCEPTED ← known points (boundary conditions)
TRIAL ← known points (boundary conditions)
FAR ← all other points

while TRIAL is not empty do

    X ← minimum of TRIAL
    change X from TRIAL to ACCEPTED

    for Y in neighbours of X, Y not in ACCEPTED do

        update solution in Y from X          ▷ minimum between current and new values

        if Y is in FAR then
            change Y from FAR to TRIAL
        end if

    end for

end while
```

that the signal re-enters the network a second time through a given PMJ before this PMJ is reached via propagation within the network. This also discards the possibility of higher degrees propagation.

On account of that, the solution is divided in five main steps, explained bellow and illustrated in Figure 10.

Independent solution in the Purkinje network The first step consists of solving the Eikonal equation in the Purkinje network. This solution takes the closest point to the atrioventricular node as the starting one. The propagation mechanism is straightforward for this one-dimensional, single-sourced case: the trial points are the ones consecutive to those accepted and a single evaluation, with an upwind scheme, is enough for solving the whole activation. See Figure 10a.

Independent solution in the myocardium In the case of additional sources in the myocardium – pacemakers, abnormal muscular sources or additional conduction paths –, the algorithm requires the solution of the Eikonal problem in the myocardium considering only the additional sources (Figure 10b). These can also include a signal coming from the right ventricle, for example in the case of left bundle branch block. This step is senseless if no myocardial sources are present.

Classification of the PMJ Once independent solutions in both domains are available, one can classify the PMJ as being orthodromic or antidromic, according to their activation times in each solution. Assuming d_{ortho} is the propagation delay when traversing the PMJ in the orthodromic direction and d_{anti} the delay in the antidromic one, then a PMJ positioned in point x is said to be orthodromic if $u|_{network(x)} + d_{ortho} \leq u|_{myocardium(x)} + d_{anti}$, and antidromic otherwise. In other words, a PMJ is orthodromic if the signal traversing it first comes from the network and antidromic if it arrives from the myocardium, taking into consideration the different propagation delays in each direction. For cases with no myocardial sources, all PMJ are orthodromic (see the above Hypothesis).

Final solution in the network From the classified PMJ, the next part consists of solving the activation in the network taking the antidromic PMJ as sources, in addition to the previously considered ones. After solving the Eikonal problem, the PMJ classification is updated so that PMJ activated from antidromic sources are considered (see Figure 10c).

Final solution in the myocardium The final solution in the network being known, one can proceed to the final step. It consists of solving the Eikonal problem in the myocardium taking both additional myocardial sources and orthodromic PMJ as initial points, represented in Figure 10d.

Among the contributions offered by this work, the code for simulating the electrical activation was rewritten. Some new features such as adding multiple activation sites and cleaner outputs were implemented. Also, a prominent gain in performance was obtained: runtime was reduced in about 63 % (from 52 minutes to less than 20 and, for a particular case, to less than a minute).

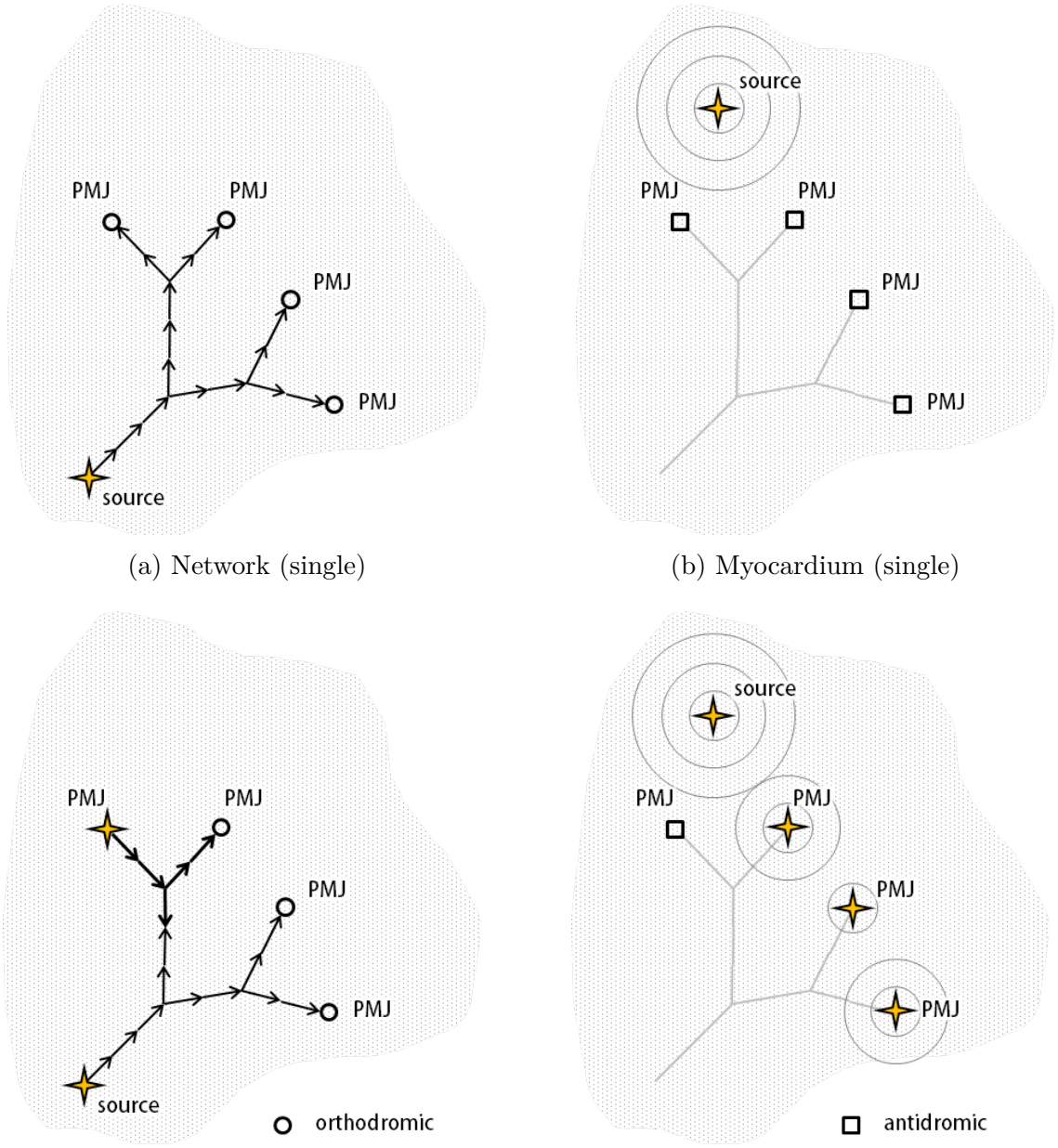

(a) Network (single)

(b) Myocardium (single)

(c) Network (coupled)

(d) Myocardium (coupled)

Figure 10: Coupling between domains

Firstly, activation times in the PMJ are obtained from the healthy source in the network (Figure a). Then, activation times due to myocardial sources are calculated (Figure b), allowing PMJ classification. Thirdly, network activation is recalculated considering antidromic PMJ as sources.

Finally, myocardial activation is recalculated considering orthodromic PMJ as sources.

4 Results

Once the geometrical model is defined and associated with the electrical activation equations, one can simulate the propagation in the ventricle by choosing the sources' locations and their respective activation times. Also, by changing configurations, one can test different scenarios and study activation patterns for a variety of healthy and pathological clinical pictures.

4.1 Simulations

Following the contextualisation provided so far, this work is mostly interested in three main cases: the activation with left bundle branch block, the healthy version of this activation and the a CRT treatment of the blocked case.

In all simulations, propagation velocity is adjusted to fit healthy activation anatomical parameters.

4.1.1 Left bundle branch block

The left bundle branch block condition is simulated by defining a region of very low conduction velocity on the septal region of the ventricle, *i.e.*, the beginning of the modellised network. As a consequence, signal coming from the regular activation path takes a longer time to arrive, and the wave front from the right ventricle plays henceforth an important role in the left ventricle's activation. The modellisation takes then into account an extra source, namely that from the right ventricle.

In the simulation results presented in Figure 11, it is possible to see that the whole activation is delayed. In particular, one can notice the late septal region affected by the bundle branch block in Figure 11b, and compare it with the healthy case simulated below (Figure 12b).

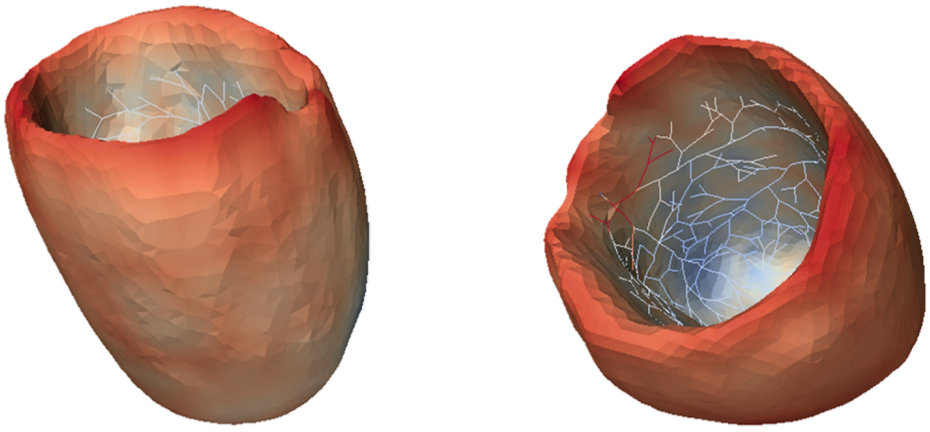

(a) (b)

Figure 11: Simulation of a left bundle branch block
One can notice the late activation on the region affected by the bundle branch block.

4.1.2 Healthy

A very interesting facility of the numerical simulation is its versatility and easiness in changing parameters. In this case, it permits simulating a hypothetical scenario of the healed pathological condition. This means that one can test how the patient's activation would behave if the pathology was not present.

Not only this simulation provides a reference activation to better understand in which aspects the pathology affects activation more, but also it constitutes an idealistic reference to be aimed by CRT optimisation.

Activation in the healthy case is triggered by the sino-atrial node and follows the anatomical path described in Section 2. It can therefore be represented by a single source on the network point closest to the atrioventricular node; no myocardial sources are present.

This sort of simulation has a particular interest for patients suffering from a conduction pathology, for it permits simulating how the activation map would be in healthy conditions.

The simulation results are shown in Figure 12. One can notice the directional character of the healthy activation, from the apex toward the base.

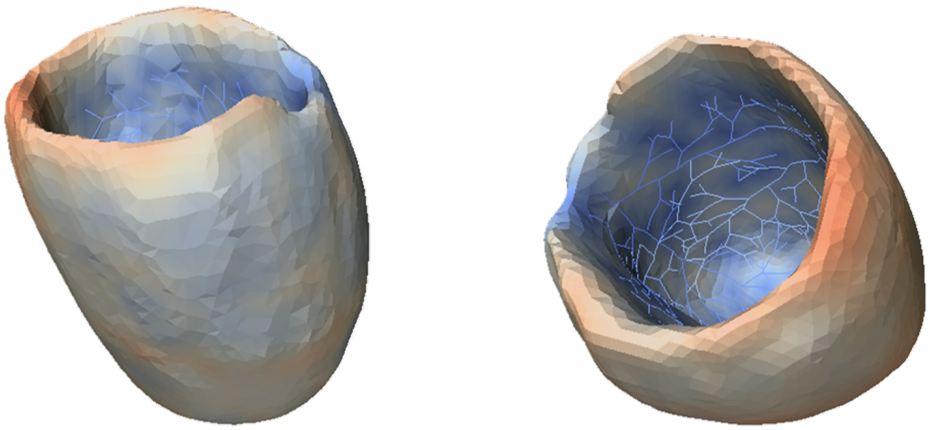

(a) (b)

Figure 12: Simulation of a healthy case

4.1.3 Resynchronised left bundle branch block

For the case analysed above (the LBBB one), one could test the effects of a CRT implantation by adding two artificial sources, positioned in accordance with Section 2. The left and right leads are positioned respectively on the apex and along the approximate region of the coronary sinus.

The criterion used by the cardiologists in Rovereto was applied to choose the best position for the left catheter. The latest point was chosen constrained to be situated within the coronary veins. The activation times were then translated in order to optimise the fit between the CRT and the Healthy curves, showed bellow in Section 4.2. Indeed, simulating a healthy condition shows itself as an useful feature, providing CRT optimisation with a reference to be aimed at.

The constraints in positioning the left lead open field to discussing alternative methods of implantation, able to access different regions of the heart's walls, since accessing high pressure chambers is not an easy procedure in practical terms (see Section 2). Ideally, a "surface lead" would wrap the whole heart and activation would be optimised point by point.

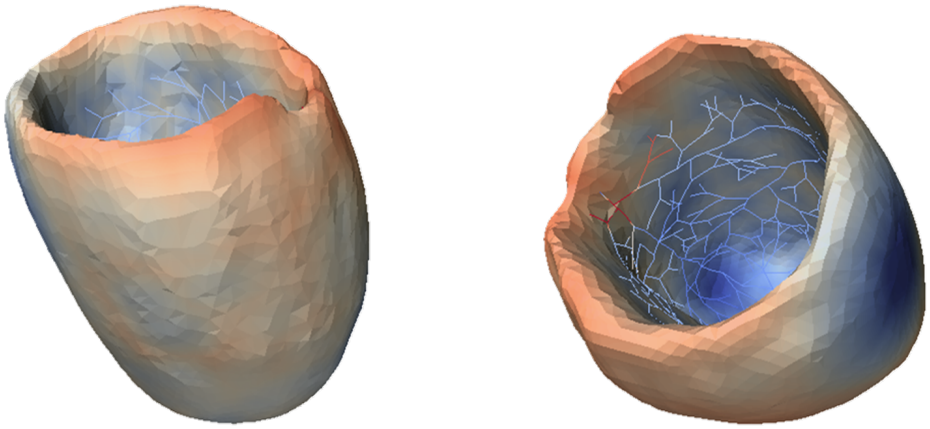

(a) (b)

Figure 13: Simulation of a resynchronised left bundle branch block

4.2 Comparison

Although Figures 11, 12 and 13 offer valuable visual information, some condensed information could be of use for comparison matters. In Figure 14, bellow, the percentage of activated tissue is plotted as a function of time for the three cases.

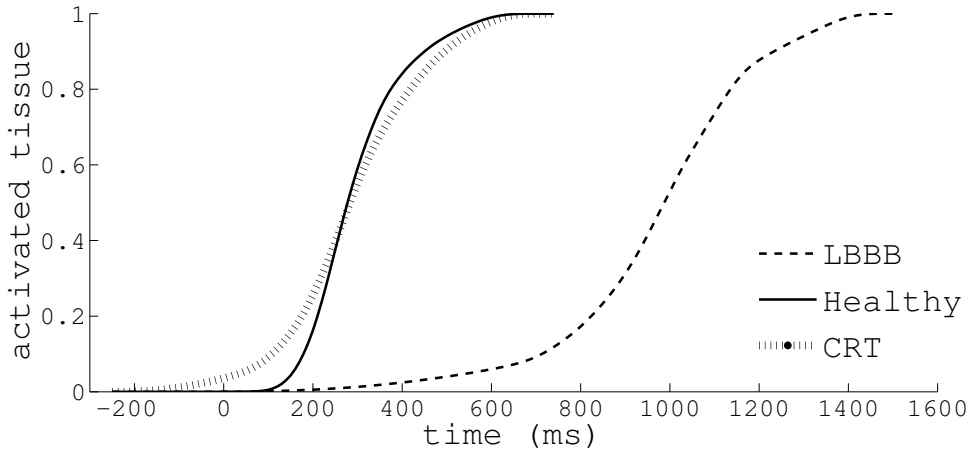

Figure 14: Comparison between cases

Taking the healthy case as a reference, one can clearly notice the large delay introduced by the left bundle branch block.

In addition, it is possible to see the benefits of CRT in recruiting muscular tissue for contraction. However, even if the treated CRT case is much closer to the healthy one, important differences in the starting and ending phases are present.

Also, one can explain the difference in slopes with the fact that healthy activation makes full use of the fibres, whilst CRT activation initiates in the muscle and inevitably takes a few moments to reach the Purkinje network. As a consequence, a longer tail is present in the beginning of the curve.

5 Conclusion

Gathering information from the bibliography, the discussions with the clinicians, and an overview of CRT research, it is possible to affirm that this is a prominent field, even if full of complicated steps to be overcome.

Above all, studies being conducted nowadays are highly dependent of invasive clinical data. In this area the great challenge for scientists in the next years is, in the one hand, to make clinical analyses less invasive and more precise and, on the other hand, to reduce the amount of information required by reliable cardiac simulations aiming the CRT.

Ideally, the development of algorithms and softwares will be able to provide clinicians with pertinent information on the patient's health conditions *prior to the intervention*, aiding clinicians to evaluate more precisely the need for CRT and make decisions on whether the intervention should be carried or not – the odds of its providing the desirable response, the risks, the evolution of the clinical picture and, in the pertinent case, the positioning and timing of the catheters.

For this purpose, research can already count on radiology acquisition and clinical history. Nevertheless, in what concerns the electrical part, non-invasive techniques are yet practically restrained to surface electrocardiograms. Although these can be of great use in diagnostics and a reference for the effectiveness of the treatment, they seem to be left aside in research and could possibly be a fruitful point to concentrate efforts on.

In the context of this work, one can also notice that only electrical behaviour is being analysed. Indeed, although this approach is more feasible and fulfils the needs of the study, a fully precise model of the heart should count with its mechanical behaviour – in particular for cases of infarction scars and non-homogeneous contraction.

In resume, the conducted work made contributions the previous studies of Palamara [2014] and Savaré [2014] on CRT: the simulation codes were optimised, new features were added, as well as a new script for image inpainting.

The study also started off the analyses including EnSite NavX technology, that seems to be the future in what concerns the CRT electrical analyses, since complete endocardial maps are riskier approaches and are not of great use for the new clinical approaches.

Finally, the work would not be complete if it had not raised discussions on the goals and possibilities of CRT research, the needs and methods of the clinicians and a little part of future of cardiology.

References

Blanc, J.-J., Etienne, Y., Gilard, M., Mansourati, J., Munier, S., Boschat, J., Benditt, D. G., and Lurie, K. G. (1997). Evaluation of different ventricular pacing sites in patients with severe heart failure results of an acute hemodynamic study. *Circulation*, 96(10):3273–3277.

Blender Online Community (2015). *Blender - a 3D modelling and rendering package*. Blender Foundation, Blender Institute, Amsterdam.

Butter, C., Auricchio, A., Stellbrink, C., Schlegl, M., Fleck, E., Hörsch, W., Huvelle, E., Ding, J., Kramer, A., in Congestive Heart Failure II Study Group, P. T., et al. (2000). Should stimulation site be tailored in the individual heart failure patient? *The American journal of cardiology*, 86(9):K144–K151.

Faggiano, E., Lorenzi, T., and Quarteroni, A. (2014). Metal artefact reduction in computed tomography images by a fourth-order total variation flow. *Computer Methods in Biomechanics and Biomedical Engineering: Imaging & Visualization*, (ahead-of-print):1–12.

Ijiri, T., Ashihara, T., Yamaguchi, T., Takayama, K., Igarashi, T., Shimada, T., Namba, T., Haraguchi, R., and Nakazawa, K. (2008). A procedural method for modeling the purkinje fibers of the heart. *The Journal of Physiological Sciences*, 58(7):481–486.

Kerckhoffs, R. C., Faris, O. P., Bovendeerd, P. H., Prinzen, F. W., Smits, K., McVeigh, E. R., and Arts, T. (2003). Timing of depolarization and contraction in the paced canine left ventricle: model and experiment. *J. Cardiovasc. Electrophysiol.*, 14(10 Suppl):S188–195.

Konukoglu, E., Sermesant, M., Clatz, O., Peyrat, J.-M., Delingette, H., and Ayache, N. (2007). A recursive anisotropic fast marching approach to reaction diffusion equation: Application to tumor growth modeling. In *Information processing in medical imaging*, pages 687–699. Springer.

Netter, F. and Yonkman, F. (1981). *Cuore*. Atlante di anatomia, fisiopatologia e clinica. Ciba-Geigy edizioni.

Palamara, S. (2014). *Numerical approximation of the electrical activity in the left ventricle with the inclusion of the Purkinje fibers*. PhD thesis, Politecnico di Milano.

Palamara, S., Vergara, C., Catanzariti, D., Faggiano, E., Pangrazzi, C., Centonze, M., Nobile, F., Maines, M., and Quarteroni, A. (2014). Computational generation of the Purkinje network driven by clinical measurements: the case of pathological propagations. *Int J Numer Method Biomed Eng*, 30(12):1558–1577.

Reumann, M., Farina, D., Miri, R., Lurz, S., Osswald, B., and Dössel, O. (2007). Computer model for the optimization of av and vv delay in cardiac resynchronization therapy. *Medical & Biological Engineering & Computing*, 45(9):845–854.

Romero, D., Sebastian, R., Bijnens, B. H., Zimmerman, V., Boyle, P. M., Vigmond, E. J., and Frangi, A. F. (2010). Effects of the purkinje system and cardiac geometry on biventricular pacing: a model study. *Ann Biomed Eng*, 38(4):1388–1398.

Savaré, S. (2014). Studio computazionale di ottimizzazione della stimolazione nella terapia di risincronizzazione cardiaca. Master's thesis, Politecnico di Milano.

Sethian, J. A. (1999). Fast marching methods. *SIAM Rev.*, 41(2):199–235.

Tobon-Gomez, C., Duchateau, N., Sebastian, R., Marchesseau, S., Camara, O., Donal, E., De Craene, M., Pashaei, A., Relan, J., Steghofer, M., Lamata, P., Delingette, H., Duckett, S., Garreau, M., Hernandez, A., Rhode, K. S., Sermesant, M., Ayache, N., Leclercq, C., Razavi, R., Smith, N. P., and Frangi, A. F. (2013). Understanding the mechanisms amenable to CRT response: from pre-operative multimodal image data to patient-specific computational models. *Med Biol Eng Comput*, 51(11):1235–1250.

Vergara, C., Palamara, S., Catanzariti, D., Nobile, F., Faggiano, E., Pangrazzi, C., Centonze, M., Maines, M., Quarteroni, A., and Vergara, G. (2014). Patient-specific generation of the Purkinje network driven by clinical measurements of a normal propagation. *Med Biol Eng Comput*, 52(10):813–826.

Yu, C. M., Wing-Hong Fung, J., Zhang, Q., and Sanderson, J. E. (2005). Understanding nonresponders of cardiac resynchronization therapy–current and future perspectives. *J. Cardiovasc. Electrophysiol.*, 16(10):1117–1124.

Yushkevich, P. A., Piven, J., Cody Hazlett, H., Gimpel Smith, R., Ho, S., Gee, J. C., and Gerig, G. (2006). User-guided 3D active contour segmentation of anatomical structures: Significantly improved efficiency and reliability. *Neuroimage*, 31(3):1116–1128.